Effect of annealing on structure and superconducting properties in Fe(Se,Te)

Journal of Physics: Conference Series **1559** (2020) 012053 doi:10.1088/1742-6596/1559/1/012053

Effect of annealing on structure and superconducting properties in Fe(Se,Te)

A. Masi[1,2], C. Alvani[2], A. Angrisani Armenio[2], A. Augieri[2], G. Celentano[2], G. De Marzi[2], C. Fiamozzi Zignani[2], F. Fabbri[2], A. La Barbera[2], F. Padella[2], F. Rizzo[2], E. Silva[1], A. Vannozzi[2]

[1] Università degli studi di Roma Tre, Roma 00146, Italy
[2] ENEA, Roma 00196, Italy

andrea.masi@uniroma3.it

Abstract. In this paper, the effect of post synthesis annealing treatments on a Fe(Se,Te) polycrystalline material is evaluated and discussed. The samples have been obtained via melting route. The material has been subjected to a high-temperature annealing treatment, carried out for 45 h at 680 °C. The role of the cooling step was investigated comparing samples obtained after a controlled cooling or after quenching in liquid nitrogen. From a morpho-structural point of view, the annealing treatment improves homogeneity, with respect to pristine samples, and influences secondary phase precipitate morphology. Regarding superconducting properties, a key role of the cooling procedure is assessed: controlled cooling leads in fact to a significant improvement of high field behaviour with respect to the melted material, while quenched samples are characterized by a worsening of the superconducting properties. Despite the overall worsening, however, the quenched samples show evidence of the presence of superconducting phases characterized by a remarkably high critical temperature (T_c > 18 K), observed for these materials only in films or under pressure.

1. Introduction

The discovery of high temperature superconductivity in iron based compounds [1] has led to significant efforts in the synthesis of these compounds, thanks to the large critical fields and high critical currents that this class of materials exhibits [2,3]. Several groups of Iron Based Superconductor (IBSC) compounds have been discovered: these materials share a common structural element, namely a layer composed by a square lattice of Fe in tetrahedral coordination with pnictides (P, As) or chalcogen (S, Se, Te) atoms. The different structures are then originated intercalating atoms, ions or molecules between the layers.

The Fe(Se,Te) system, the foremost exponent of "11" family [6,7], characterized by a simple structure among IBSC and lower toxicity with respect to As-containing compounds, is considered interesting for low-temperature/high-field applications thanks to its high critical fields and critical current densities. The properties of Fe(Se,Te) superconducting materials have been evaluated by several groups, targeting polycrystalline materials, films and single crystals [7]. However, both Fe-Se and Fe-Te system are characterized by complex phase diagrams [8,9] and no ternary phase diagram has been assessed. To complicate the matter, beside the Se:Te ratio, superconducting properties of Fe(Se,Te) system have been linked interstitial iron atoms in the tetragonal lattice [10], a lattice defect

that stabilizes tetragonal phase for high Te content. These two issues lead to a difficult interpretation of results reported in literature for similar compositions processed through different methods [7]. The uncertainties are furthermore enhanced by the reports of multiple phases [11–15] or chemical inhomogeneities [16–18] reported for single crystals, supposed to play a role on superconducting properties [19,20].

In this context, the role of the cooling from high temperature, in particular, and its influence on morpho-structural and physical properties can be elusive [21]. In our recent work, we observed that synthesis of Fe(Se,Te) through melting routes leads to the presence of multi-phase Se-rich precipitates in a superconducting tetragonal matrix independently of the cooling rate [22]. A subsequent long-term high temperature (680 °C) annealing of melted samples does not lead to the decrease or vanishing of these precipitates, suggesting their stability at 680 °C [23].

In this paper, the effect of a shorter post synthesis annealing treatments on the materials properties is evaluated and discussed, and the role of the cooling step on morpho-structural and physical properties is investigated and assessed. Bulk solid samples have been obtained through a melting route and have been characterized by means of X-Ray diffraction and electron microscopy analysis. Superconducting properties have been evaluated by means of electrical and magnetic measurements.

2. Experimental

Polycrystalline Fe(Se,Te) samples were obtained by a melting method as in [23]. Briefly, powder mixtures with Fe:Se:Te=1:0.5:0.5 at% (Fe from Sigma Aldrich, >99%, Se from Sigma Aldrich, 99.99% and Te from Sigma Aldrich, 99.8%) were compressed into pellets and sealed in vacuum in quartz vials. The vials were heated up to 1000 °C (1 °C/min) for 4 h and successively cooled to room temperature (5 °C/min cooling rate). After the synthesis step, the vials were heated at 680 °C for 45 h. After this period, one of the vials was extracted from the furnace and quenched in liquid nitrogen (quenched sample), while the other was cooled with a 5 °C/min ramp (controlled cooling sample).

X-Ray Diffraction (XRD) analysis was carried out on pulverised samples in a Seifert PAD VI instrument equipped with a Cu tube and a graphite monochromator on the diffracted beam. Pseudo-Voigt functions were used to fit peak profiles [24]. Morphological and compositional analysis was carried out on polished sections with a Leo 1525 Scanning Electron Microscope (SEM) equipped with Oxford x-act energy dispersive spectroscopy (EDS) system. Superconducting characterization was carried out by means of electrical and magnetic measurements. Electrical resistance was measured using a standard four contacts method on small disks (Ø≈5 mm, h≈1.2 mm) cut from the solid. Magnetic measurements were performed by means of an Oxford Instrument Vibrating Sample Magnetometer (VSM) on the same samples. Measurements were carried out with the field applied perpendicularly to the disk surface. Direct Current (DC) magnetization was measured in Zero Field Cooling (ZFC) and Field Cooling (FC) conditions applying a 0.002 T magnetic field.

3. Results and discussion

The results of XRD analysis are reported in Figure 1. Both samples exhibit similar multi-phase patterns. Main peaks are ascribable to a β-Fe(Se,Te) tetragonal phase. Minor peaks are ascribable to a hexagonal-like phase (e.g. δ-FeSe, Fe_7Ch_8 or Fe_3Ch_4 [8,9]), characterized by a shift with respect to reference positions most likely due to the presence of the mixed chalcogens in the lattice. It is not possible to discriminate between a pure hexagonal NiAs phase or its distorted deriving phases (i.e. Fe_7Ch_8 or Fe_3Ch_4) commonly observed in Fe-Se and Fe-Te systems due to the high similarity of the patterns. Comparing the hexagonal-like phase peaks, a slight difference in the position (see inset c of Figure 1) can be observed between the two samples, indicating a small difference in the lattice parameters. Furthermore, a higher peak intensity in the quenched pattern is evident, likely ascribable to a higher relative content of this phase.

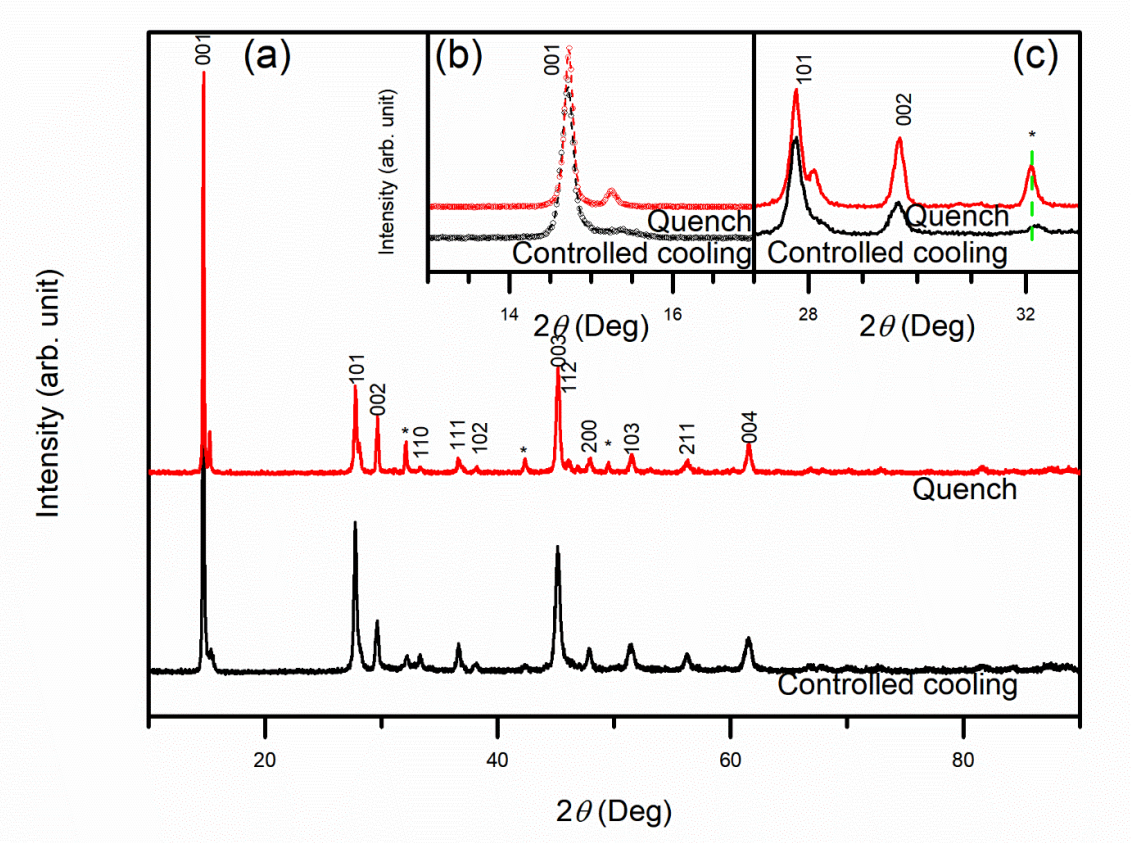

Figure 1. (a) XRD patterns of the two samples. Numerical labels indicate reflections ascribable to a β-Fe(Se,Te) tetragonal phase, while * indicate peaks ascribable to a secondary Fe_7Se_8-like phase; (b), detail of the 001 peak (empty circles) with over imposed pseudo-Voight fit (dashed lines); (c) detail of the experimental patterns in the 27-33 ° region, showing the shift of the Fe_7Se_8-like phase peak.

Observing in detail the tetragonal phase peaks, a high angle shoulder or in some cases peak splitting is observable. This evidence, reported in particular for the 001 reflection in the inset b of Figure 1, suggests the presence of multiple tetragonal phases characterized by a different chemical composition. Se:Te ratio influences in fact significantly lattice parameter *c* [6], often taken as reference to evaluate chemical composition and homogeneity in these materials [21]. To further analyze this result, the 001 peak was fitted with two pseudo-Voigt functions, to consider respectively the main peak and the high angle component. The results of the analysis are reported in Table I. Both samples are characterized by a similar position of the two peaks, while a significant difference can be observed instead in the peak width values. This suggests that both samples are characterized by the presence of tetragonal phases with similar average Se:Te ratio, and that these phases are characterized by a higher chemical homogeneity in the quenched sample.

Table I: position (2θ) and Half Width at Half Maximum (HWHM) of the β-Fe(Se,Te) 001 reflection peaks as obtained by pseudo-Voight fits:

Sample	Peaks	2θ (°)	HWHM (°)
Controlled cooling	Main peak	14.71	0.09
	High angle component	15.22	0.37
Quench	Main peak	14.73	0.06
	High angle component	15.26	0.07

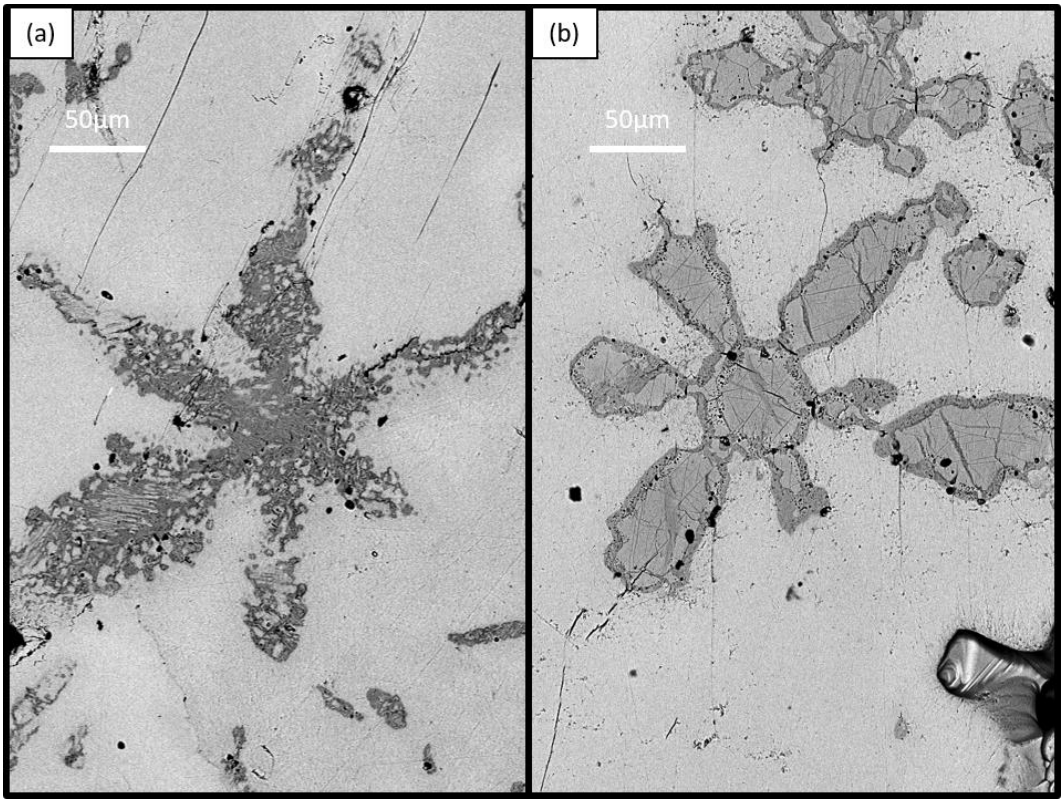

Figure 2. SEM images (back-scattered electrons) of the controlled cooled (a) and of the quenched (b) samples polished sections.

The morphology of the sample sections is depicted in Figure 2. Both samples are characterized by the presence of dendritic precipitates of similar shape in a matrix, confirming what previously observed in sample obtained by similar melting routes [22,23].

Observing in detail the precipitate morphology, reported in Figure 3, the images allow to distinguish in both sample similar phases: the light grey matrix (A), and a dark (B) and an intermediate grey region (C) in the precipitates. The fine morphology of the precipitates is different between the two samples: the controlled cooled sample is characterized by the presence of smooth and curved lamellae of the alternated B and C phases. The quenched sample precipitates exhibit a dark grey defined border region and dark grey needle like structures that respectively surround and intersect the intermediate grey region.

To gain further insight on the observed morphological features, EDS analyses were carried out on the different areas, and the results are summarized in Figure 4. As evident by the figure, the three different regions are characterized in both samples by similar compositions. Regions A and B possess a Fe:Chalcogen ratio ≈1, indicating a tetragonal structure, while region C is characterized by an iron deficiency, compatible with a Fe_7Ch_8 composition. The matrix is rich in tellurium (Se:Te~ 0.8), while the precipitates (region B and C) are characterized by a Se enrichment (Se:Te ~2.5).

The correlation between XRD and SEM/EDS results, to define the samples structure and composition, is quite straightforward. The matrix A corresponds to the main tetragonal phase, with B regions responsible for the high angle component of the tetragonal phase diffraction peaks. C regions, as suggested by its chemical composition, correspond finally to the hexagonal-like phase.

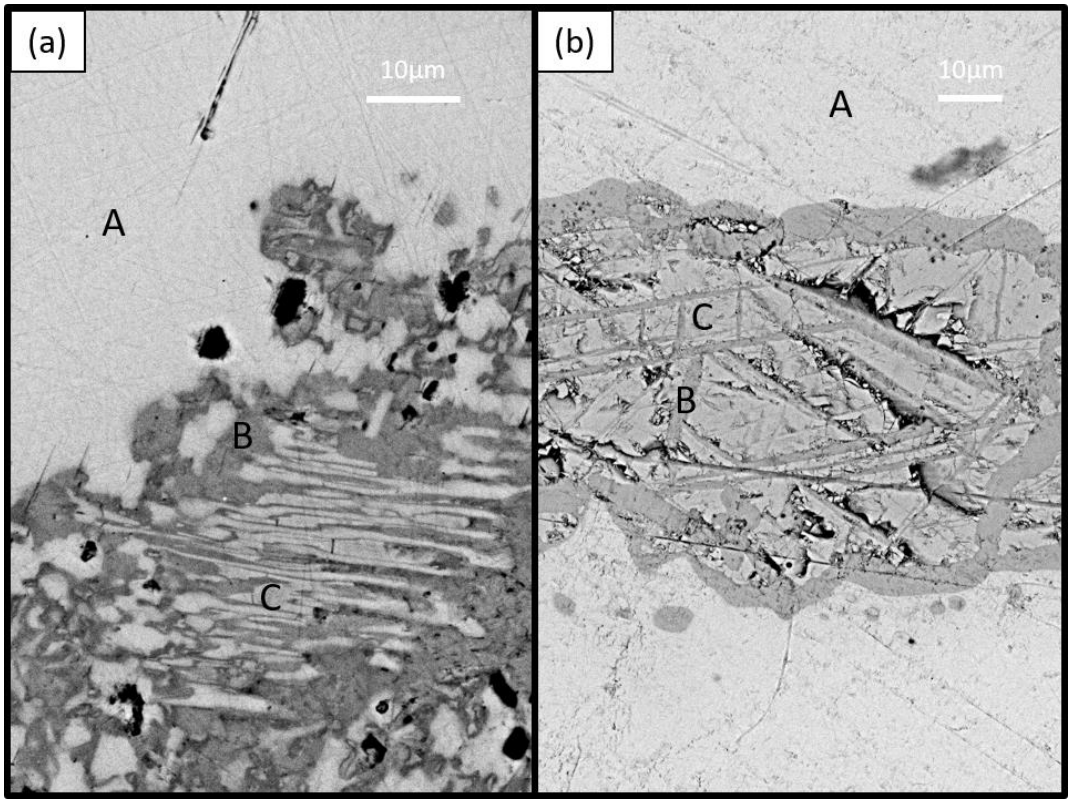

Figure 3. SEM images (back scattered electrons) of the details of the precipitates in the (a) controlled cooled and (b) quenched samples. A, B and C mark three different regions corresponding to the matrix (A) and to the precipitates tetragonal (B) and hexagonal (C) phases respectively.

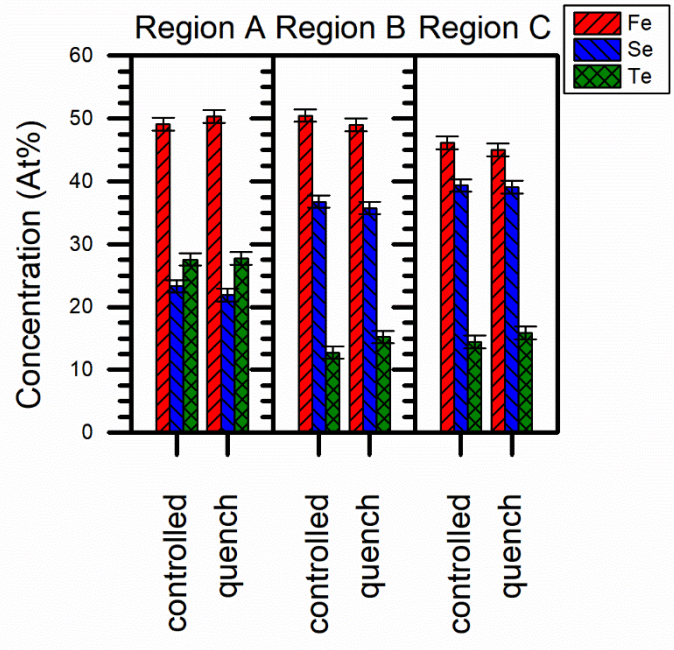

Figure 4. Summary of the results of EDS analyses carried out on the different samples regions (see text for details).

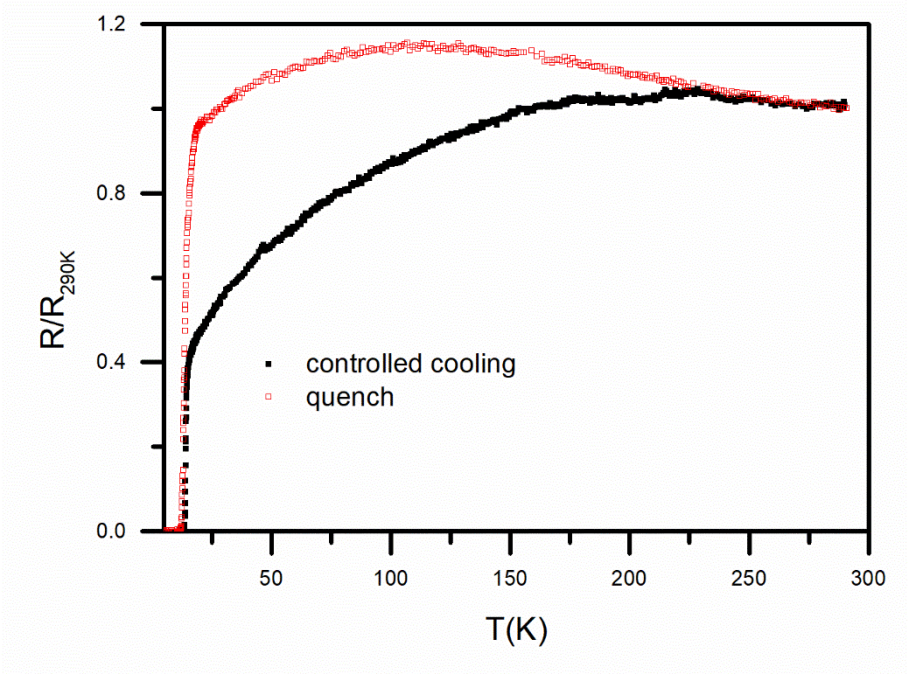

Figure 5. electrical resistance as a function of the temperature.

The electrical behaviour of the samples is depicted in Figure 5. Both samples are characterized by an initial moderate rise of the electrical resistance when cooling down from room temperature, and a metallic behaviour ($dR/dT>0$) at lower temperature, with some differences in the temperature corresponding to the maximum of the curves, respectively approximately 150 K and 100 K for the controlled cooled and quenched samples. At low temperature, both samples exhibit a superconducting transition.

The detail of the superconducting transition is reported in Figure 6. As evident in Figure 6a, the controlled cooled sample is characterized by a linear decrease down to approximately 15 K, followed by a sharp decrease of the electrical resistance, with a zero critical temperature of approximately 13.6 K. The quenched sample instead shows a broad and multi-step superconducting transition. The derivative of the electrical resistance is reported in Figure 6b. Comparing the curves, it can be observed the sharpness of the controlled cooling sample transition, and the multi-modal nature of the transition of the quenched sample. The latter is in fact characterized by a high temperature shoulder and a main peak at around 13 K. Considering the high temperature part, the resistance starts to decrease at approximately 19 K, and a significative portion of resistance drop is observed already above 16 K.

In the case of the controlled cooled sample the superconducting phase responsible of the measured electrical transition is the matrix, with the tetragonal phases of region B characterized by a lower T_c [23]. The case of the quenched sample seems different: as we observed previously, a high temperature quench process causes a worsening of the critical temperature of a melted sample [22], with a zero resistance temperature that drops from 14 K to less than 12 K. In the quenched sample we can recognize this effect on the matrix. In our previous quench studies, carried out directly on melted samples, we couldn't observe however such a high transition onset: this indicates that the annealing treatment plays a key role in this. The presence of high T_c superconducting phases occurs therefore when a high degree of homogeneity, induced by the high temperature annealing, is coupled to a rapid cooling step.

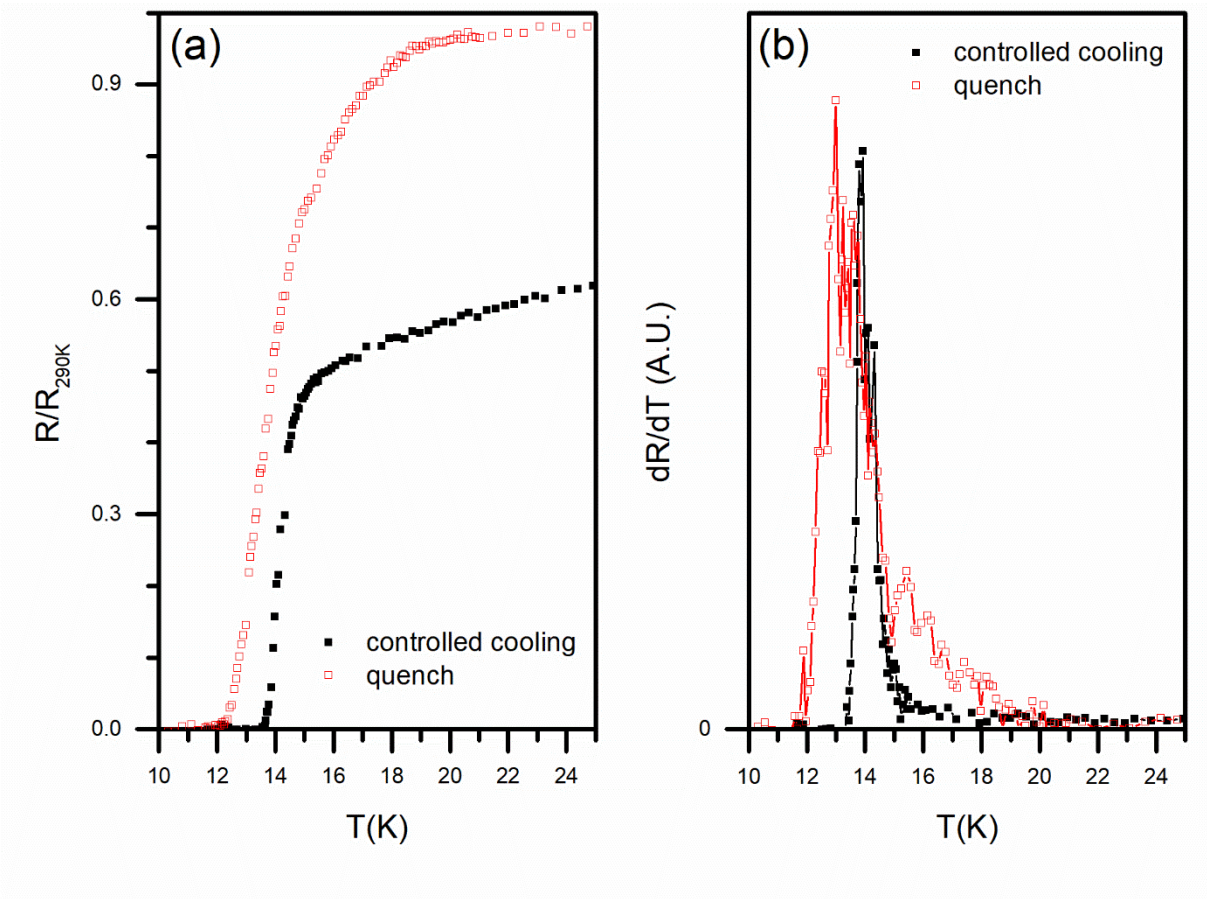

Figure 6. details of the superconducting transition: (a) electrical resistance and (b) resistance derivative as a function of temperature.

Results of the magnetic characterization are reported in Figure 7. In Figure 7a the magnetization measured in ZFC and FC conditions is depicted as a function of temperature. It can be observed that both samples exhibit a superconducting transition at low temperature. The controlled cooling sample is characterized by a dual transition, with a sharp onset at approx. 14 K and a second drop starting at approx. 8 K. The quenched sample is characterized by a smooth and broad transition and exhibits a smaller shielded volume with respect to the controlled cooling sample. The comparison between the curves shows that a slow cooling influences positively the amount of superconducting phase in the material.

The curve of the controlled cooling sample is quite similar to the one previously observed for a longer annealing treatment [23], suggesting that the structuration of the two rather distinct superconducting phases occurs during the first hours of the annealing treatment. We can assume the matrix responsible for the higher temperature superconducting transition, while the lower temperature transition is ascribable to the Se-rich tetragonal phase in the precipitates. Regarding the quenched sample, instead, a multiple superconducting transition is not observed. This suggests that the amount of volume of the superconducting phase responsible for the high onset in the resistive transition is quite small.

In Figure 7b the hysteresis loops measured at 4.2 K are reported. The controlled cooling sample is characterized by a wide and open hysteresis, with a clear fish-tail effect showing a second peak in the magnetization loop at approx. 8T. The quenched sample, on the contrary, shows a significantly narrower curve, with clear evidences of an underlying non superconducting magnetic phase.

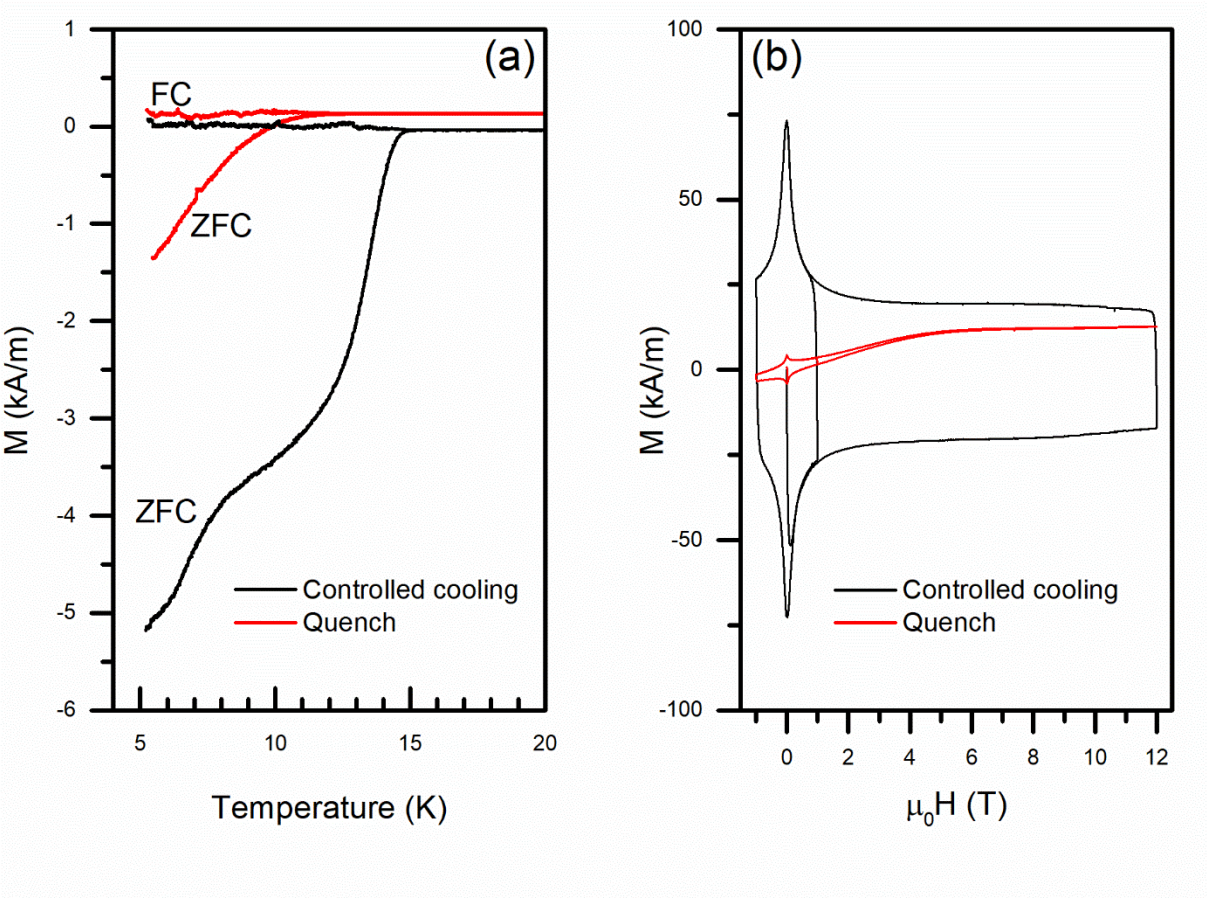

Figure 7. Results of the magnetic measurements. (a) superconducting transitions and (b) hysteresis loops at 4.2 K.

4. Conclusions

Polycrystalline samples of $FeSe_{0.5}Te_{0.5}$ (overall composition) obtained by melting methods are characterized by the presence of multi-phase Se-rich precipitates in a tetragonal Te-rich matrix. Morphology and phase composition of the precipitates are greatly influenced by a high temperature annealing treatment, and in particular by the final cooling step.

Samples obtained by a controlled cooling after a 680 °C heat treatment are characterized by the presence of smooth lamellae of alternating hexagonal and tetragonal phases, while quenching leads to tetragonal-hexagonal core-shell structure with inclusions of tetragonal needle-like features. As a further difference, quenching leads to an overall higher amount of hexagonal-like Se-rich secondary phase, suggesting that this phase is stable at high temperature and tends to decompose during the cooling.

Regarding superconducting properties, the controlled cooling leads to samples exhibiting sharp transitions and wide magnetic hysteresis loops. On the contrary, the quenched sample is characterized by broader transitions, narrow hysteresis loops and the significant presence of magnetic non superconducting phases. This suggests that the solid state reactions and rearrangements occurring during the cooling step are mandatory to achieve good superconducting properties in bulk $FeSe_{0.5}Te_{0.5}$ samples.

Finally, it is worth noting that despite the overall worse superconducting properties of the quenched sample with respect to the controlled cooling, the resistive transition of the quenched sample is characterized by an extremely high transition onset (Tc^{onset} ~ 19 K), commonly observed in Fe(Se,Te) materials only for films or under pressure. It could be assumed therefore that the quenching procedure

induces stress such to enhance the critical temperature or preserves some particular phase, stable at high temperature, characterized by this high critical temperature.

References

[1] Kamihara Y, Watanabe T, Hirano M and Hosono H 2008 Iron-based layered superconductor La[O1-xFx]FeAs (x= 0.05-0.12) with Tc = 26 K *J. Am. Chem. Soc.* **130** 3296–7
[2] Hosono H, Tanabe K, Takayama-Muromachi E, Kageyama H, Yamanaka S, Kumakura H, Nohara M, Hiramatsu H and Fujitsu S 2015 Exploration of new superconductors and functional materials, and fabrication of superconducting tapes and wires of iron pnictides *Sci. Technol. Adv. Mater.* **16** 033503
[3] Hosono H, Yamamoto A, Hiramatsu H and Ma Y 2018 Recent advances in iron-based superconductors toward applications *Mater. Today* **21** 278–302
[4] Rotter M, Tegel M and Johrendt D 2008 Superconductivity at 38 K in the iron arsenide (Ba1-xKx)Fe2As2 *Phys. Rev. Lett.* **101** 4–7
[5] Hsu F-C, Luo J-Y, Yeh K-W, Chen T-K, Huang T-W, Wu P M, Lee Y-C, Huang Y-L, Chu Y-Y, Yan D-C and Wu M-K 2008 Superconductivity in the PbO-type structure $α$-FeSe *Proc. Nat. Acad. Sci. USA* **105** 14262–4
[6] Yeh K-W, Huang T-W, Huang Y-L, Chen T-K, Hsu F-C, M. Wu P, Lee Y-C, Chu Y-Y, Chen C-L, Luo J-Y, Yan D-C and Wu M-K 2008 Tellurium substitution effect on superconductivity of the α-phase iron selenide *EPL* **84** 37002
[7] Martinelli A, Bernardini F and Massidda S 2016 The phase diagrams of iron-based superconductors: Theory and experiments *Comptes Rendus Phys.* **17** 5–35
[8] Predel B 1982 Fe-Se (Iron-Selenium) *Dy-Er – Fr-Mo* (Berlin/Heidelberg: Springer-Verlag) pp 1–4
[9] Predel B 1995 Fe-Te (Iron-Tellurium) *Dy-Er – Fr-Mo* ed O Madelung (Berlin/Heidelberg: Springer-Verlag) pp 1–4
[10] Sun Y, Yamada T, Pyon S and Tamegai T 2016 Influence of interstitial Fe to the phase diagram of Fe1+yTe1−xSe x single crystals *Sci. Rep.* **6** 32290
[11] Gresty N C, Takabayashi Y, Ganin A Y, McDonald M T, Claridge J B, Giap D, Mizuguchi Y, Takano Y, Kagayama T, Ohishi Y, Takata M, Rosseinsky M J, Margadonna S and Prassides K 2009 Structural Phase Transitions and Superconductivity in Fe 1+δ Se 0.57 Te 0.43 at Ambient and Elevated Pressures *J. Am. Chem. Soc.* **131** 16944–52
[12] Viennois R, Giannini E, van der Marel D and Cerny R 2010 Effect of Fe excess on structural, magnetic and superconducting properties of single-crystalline Fe1+xTe1−ySey *J. Solid State Chem.* **183** 769–75
[13] Bendele M, Weyeneth S, Puzniak R, Maisuradze A, Pomjakushina E, Conder K, Pomjakushin V, Luetkens H, Katrych S, Wisniewski A, Khasanov R and Keller H 2010 Anisotropic superconducting properties of single-crystalline FeSe 0.5 Te0.5 *Phys. Rev. B* **81** 1–10
[14] Tsurkan V, Deisenhofer J, Günther A, Kant C, Klemm M, Krug von Nidda H-A, Schrettle F and Loidl A 2011 Physical properties of FeSe0.5Te0.5 single crystals grown under different conditions *Eur. Phys. J. B* **79** 289–99
[15] Wittlin A, Aleshkevych P, Przybylińska H, Gawryluk D J, Dłuzewski P, Berkowski M, Puźniak R, Gutowska M U and Wiśniewski A 2012 Microstructural magnetic phases in superconducting FeTe 0.65Se 0.35 *Supercond. Sci. Technol.* **25**
[16] Sales B C, Sefat A S, McGuire M A, Jin R Y, Mandrus D and Mozharivskyj Y 2009 Bulk Superconductivity at 14 K in Single Crystals of Fe1+yTexSe1-x *Phys. Rev. B* **79** 094521
[17] Taen T, Tsuchiya Y, Nakajima Y and Tamegai T 2009 Superconductivity at Tc~14 K in single-crystalline FeTe0.61 Se0.39 *Phys. Rev. B* **80** 092502
[18] Hu H, Zuo J-M, Wen J, Xu Z, Lin Z, Li Q, Gu G, Park W K and Greene L H 2011 Phase separation in the iron chalcogenide superconductor Fe 1+ y Te x Se 1− x *New J. Phys.* **13**

053031
[19] Prokeš K, Schulze M, Hartwig S, Schäfer N, Landsgesell S, Blum C G F, Abou-Ras D, Hacisalihoglu M Y, Ressouche E, Ouladdiaf B, Büchner B and Wurmehl S 2015 Structural inhomogeneities in FeTe0.6Se0.4: Relation to superconductivity *J. Cryst. Growth* **432** 95–104
[20] Hartwig S, Schäfer N, Schulze M, Landsgesell S, Abou-Ras D, Blum C G F, Wurmehl S, Sokolowski A, Büchner B and Prokeš K 2018 Inhomogeneities and superconductivity in poly-phase Fe-Se-Te systems *Physica B* **531** 102–9
[21] Bhatia V, Rodriguez E E, Butch N P, Paglione J and Green M a 2011 Phase separation and superconductivity in Fe1+xTe0.5Se0.5 *Chem. Commun.* **47** 11297
[22] Masi A, Alvani C, Augieri A, Bellusci M, Celentano G, De Marzi G, Fabbri F, Fiamozzi Zignani C, La Barbera A, Padella F, Pentimalli M, Silva E, Vannozzi A and Varsano F 2018 Phase Separation and Microstructure in Superconducting FeSe1-xTex Materials *IEEE Trans. Appl. Supercond.* **28** 7300305
[23] Masi A, Alvani C, Augieri A, Bellusci M, Celentano G, De Marzi G, Fabbri F, Fiamozzi Zignani C, La Barbera A, Padella F, Pentimalli M, Silva E, Vannozzi A and Varsano F 2019 Fe(Se,Te) From Melting Routes: Insight on Phase Separation *IEEE Trans. Appl. Supercond.* **29** 7300304
[24] Wertheim G K, Butler M A, West K W and Buchanan D N E 1974 Determination of the Gaussian and Lorentzian content of experimental line shapes *Rev. Sci. Instrum.* **45** 1369–71